

# Optically active components and light attenuation in an offshore station of Harima Sound, eastern Seto Inland Sea, Japan

Hitomi Yamaguchi · Ryo Katahira ·  
Kazuhiko Ichimi · Kuninao Tada

Received: 25 January 2013 / Revised: 20 March 2013 / Accepted: 4 April 2013 / Published online: 24 April 2013  
© Springer Science+Business Media Dordrecht 2013

**Abstract** In the eastern Seto Inland Sea, Japan, phytoplankton abundance in the surface water has gradually declined, whereas Secchi depth has risen in recent years, particularly in offshore areas. Therefore, it may be hypothesized that phytoplankton dominate light attenuation in the offshore area, and that other constituents are less important. To test this hypothesis, we examined the roles of seawater, colored dissolved organic matter (CDOM), non-algal particles (tripton), and phytoplankton in the light attenuation at an offshore station of Harima Sound in the eastern Sea. The magnitude of light attenuation was then determined from the attenuation coefficient of photosynthetically available radiation (PAR) through the water column ( $K_d$ ). During a 13-month period,  $K_d$  ranged from 0.179 to 0.507  $\text{m}^{-1}$ , with a mean of 0.262  $\text{m}^{-1}$ . The mean relative contributions of seawater (15%) and CDOM (13%) to  $K_d$  were small, while the most dominant  $K_d$  constituent was tripton (45%). The mean contribution of phytoplankton to  $K_d$  (27%) was

consequently less than that of tripton. However, 75% of the temporal variability in  $K_d$  was attributed to phytoplankton, measured as chlorophyll *a*. Our results emphasize that the main component of light attenuation does not always govern the temporal variation of light attenuation in coastal regions.

**Keywords** Photosynthetically available radiation (PAR) · Light attenuation · Colored dissolved organic matter · Tripton · Phytoplankton

## Introduction

Photosynthetically available radiation (PAR), the total radiation of wavelengths between 0.4 and 0.7  $\mu\text{m}$ , is the energy source for plant photosynthesis (Parsons et al., 1984; Kirk, 2011). Underwater PAR is attenuated exponentially in the vertical plane, and diminishes as it passes through the water column. In aquatic ecosystems, the layer that is exposed to sufficient PAR for photosynthesis is consequently restricted, and the survival and distribution of both benthic and pelagic plants are influenced by the PAR availability. Knowledge of the changes and underlying mechanism of underwater PAR attenuation is therefore meaningful for understanding the function and structure of coastal areas as habitat for primary producers (McMahon et al., 1992; Philips et al., 1995; Gallegos & Moore, 2000; Yamaguchi et al., 2007; Obrador & Pretus, 2008).

---

Handling editor: Luigi Naselli-Flores

---

H. Yamaguchi (✉) · R. Katahira · K. Tada  
Faculty of Agriculture, Kagawa University, 2393 Ikenobe,  
Miki, Kita 761-0795, Japan  
e-mail: hitomiyjp@yahoo.co.jp

K. Ichimi  
Seto Inland Sea Regional Research Center, Kagawa  
University, 4511-15 Kamano, Aji, Takamatsu 761-0130,  
Japan

The magnitude of light attenuation in the water column conveys the vertical attenuation coefficient for downward irradiance of PAR ( $K_d$ ), which is an apparent optical property (cf. Kirk, 2011). Kirk (2011) summarized  $K_d$  values in various coastal and estuarine waters, which are obtained by summation of the spectral distribution data across the photosynthetic range, and noted that  $K_d$  varied from less than 0.1 to over  $10\text{ m}^{-1}$ . These values are equivalent to water depths with 1% of the surface PAR ranging between <0.5 and >46 m. Several components are responsible for PAR attenuation in the water column, and are typically divided into four categories: seawater, colored dissolved organic matter (CDOM), non-living organic and inorganic material (tripton), and phytoplankton (cf. Pfannkuche, 2002; Branco & Kremer, 2005; Kelble et al., 2005). In estuarine and coastal waters, both the quantity and quality of CDOM (Foden et al., 2008; Suksomjit et al., 2009), tripton (Pfannkuche, 2002; Kelble et al., 2005), and phytoplankton (Cloern et al., 1985; Monbet, 1992) fluctuate in time and space, because of the effects of freshwater and/or oceanic water inflows, and sediment resuspension. Hence, the relative importance of each optical component for PAR attenuation is variable, and they can all potentially contribute significantly to PAR attenuation.

At our study area, Harima Sound, in the eastern Seto Inland Sea in Japan, Secchi depth is regularly monitored as an index of water clarity. Based on Manabe et al. (1994) and Nishikawa et al. (2010), typical levels are around 5–8 m throughout the year. In contrast, high Secchi depth levels of nearly 15 m have been sporadically observed in the offshore area (Fujiwara, 2010). Although Harima Sound underwent cultural eutrophication, water quality has recently been improved because of reductions in terrestrial nitrogen and phosphorus loading (Yamamoto, 2003). Nishikawa et al. (2010) analyzed phytoplankton variability in Harima Sound from the early 1970s to the present, and reported that the annual mean value in the surface water has decreased. The Association for the Environmental Conservation of the Seto Inland Sea (2010) noted that the number of red tides has reduced to one-third (*ca.* 20 cases  $\text{y}^{-1}$ ) of its peak in 1974. Therefore, it may be hypothesized that phytoplankton dominate light attenuation in the offshore area, and other constituents are less important.

To test the aforementioned hypothesis, in this study, we examined the roles of phytoplankton, seawater, colored dissolved organic matter (CDOM), and non-algal particles (tripton) in PAR attenuation in an offshore station of Harima Sound. During a 13-month period, we focused on the following two questions: (1) how did the respective optically active components contribute to PAR attenuation, and (2) what is the main cause of temporal variation in PAR attenuation.

## Materials and methods

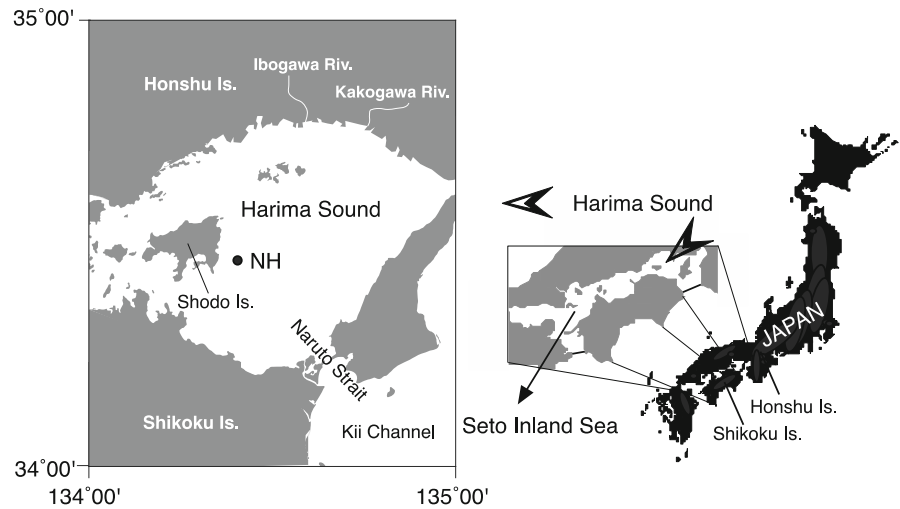
### Study area

Harima Sound has a surface area of 3,400  $\text{km}^2$ , and a mean depth of 26 m (Fig. 1). The northern coasts have relatively turbid and low salinity waters (i.e., surface salinity <30) due to freshwater inflows from the large rivers (e.g., Kakogawa and Ibogawa River). In contrast, the southeastern area around Naruto Strait has relatively clear waters and high salinities (i.e., surface salinity >33) due to inputs of oceanic waters from the North Pacific through Kii Channel. A large part of the Sound thus has characteristics reflecting its transition between estuarine and shelf waters, and surface salinity typically varies between 30 and 33 throughout the year (Manabe et al., 1994; Nishikawa et al., 2010). Our sampling station was located in the central part of Harima Sound (Stn NH; 34°28'N, 134°24'E) (Fig. 1), approximately 6 km off Shodo Island, with a mean depth of 34 m.

### Field measurements and sampling

We conducted monthly observations at Stn NH from January 2011 to January 2012. Each time, Secchi depth was measured using a Secchi disk. In parallel, vertical profiles of temperature, salinity, and downwelling PAR (wavelengths from 400 to 700 nm) were measured using a CTD equipped with an underwater quantum sensor (JFE Advantec, AAQ-1183). The CTD data were obtained from the sunny side of the vessel. The depth profiles of PAR intensity in the water followed a significantly ( $r^2 \geq 0.97$ ,  $P < 0.01$ ) exponential decrease. We thus determined  $K_d$  ( $\text{m}^{-1}$ ) based on the Lambert–Beer Law, using a least squares fit. The Lambert–Beer Law is expressed as follows:

**Fig. 1** Geographical and sampling location of the study site, Harima Sound, eastern Seto Inland Sea, Japan



$$I_z = I_0 \exp(-K_d z) \quad (1)$$

where  $z$  denotes the depth in meters, and  $I_0$  and  $I_z$  are PAR intensity ( $\mu\text{mol m}^{-2} \text{s}^{-1}$ ) below the water surface and at  $z$ , respectively. In order to calculate the depth where the PAR has been reduced to 1% of the surface value ( $Z_{\text{eu}}$ ), Eq. (1) was arranged as follows:

$$Z_{\text{eu}} = 4.61/K_d \quad (2)$$

$K_d$  is an apparent optical property, and thus depends on the aquatic medium as well as the ambient light field, including factors such as cloud status and solar elevation (Kirk, 2011). We did not record cloud status quantitatively in the present study. To evaluate the influence of solar elevation on  $K_d$ , we calculated the cosine of the zenith angle of the refracted solar beam just below the water surface,  $\mu_0$  (cf. McPherson & Miller, 1994), based on the geographic location and sampling date and time. The  $\mu_0$  at each sampling time ranged between 0.69 and 0.94, and was within a narrow range, 0.74–0.89, in almost all cases (10 of 13). For such reasons, we regarded the  $K_d$  as the quasi-inherent optical property (cf. Baker & Smith, 1979), and did not adjust the  $K_d$  data with changes in the incident radiation field.

After CTD measurements, we collected seawater samples from five depths (0, 5, 10, 20, and 30 m) using a Van Dorn water sampler. These samples were analyzed for CDOM absorbance and concentrations of chlorophyll *a* (Chl *a*) and total suspended solids (TSS).

## Analytical methods

Seawater samples for CDOM analysis were gently filtered through pre-combusted Whatman GF/F filters, and kept in amber glass bottles. Absorbances at 750 and 440 nm of the filtrated seawater were thereafter measured using a double beam spectrophotometer (JASCO, V-630). We calculated the absorption coefficients of the filtered seawater at 440 nm ( $\text{CDOM}_{440}$ ), an index of relative abundance of CDOM (Kirk, 2011), using the following equation (Lund-Hansen, 2004; Lund-Hansen et al., 2010a):

$$\text{CDOM}_{440} = 2.303(\text{ABS}_{440} - \text{ABS}_{750})/L \quad (3)$$

where  $\text{ABS}_{440}$  and  $\text{ABS}_{750}$  are the absorbance at 440 and 750 nm, respectively, and  $L$  is the cuvette length in meters ( $=0.1$ ).

We used Whatman GF/F filters (0.7  $\mu\text{m}$  pore size) for CDOM determination, although filters with a nominal pore size of 0.2  $\mu\text{m}$  are recommended and used in many recent CDOM studies to remove all particles from water samples (Laanen et al., 2011). According to previous studies, the increase in CDOM absorption due to the addition of sub-micron (0.2–0.7  $\mu\text{m}$ ) particles is estimated to be around 10% (Branco & Kremer, 2005; Laanen et al., 2011) or lower (Nelson et al., 1998) on average, in field studies. Thus, our measurements of  $\text{CDOM}_{440}$  will be slightly overestimated, mainly due to the scattering effect of sub-micron particles. However, we do not feel that this overestimation of the  $\text{CDOM}_{440}$  has substantially affected our conclusions.

For the analysis of Chl *a*, a known volume of seawater samples was filtered through Whatman GF/F filters. These filters were soaked in 90% acetone, stored in darkness at 5°C for a day, and supersonic treatment was thereafter performed to promote pigment extractability. The acetone extracts were passed through PTFE Ekicrodisk filters (0.45 µm pore size) to reduce the turbidity from particles. Pigments extracted in the acetone were determined by the trichromatic spectrophotometric method (Jeffrey & Humphrey, 1975).

For the analysis of TSS, 1,500–2,000 ml of seawater samples was passed through pre-weighted and pre-combusted Whatman GF/F filters. These filters were rinsed in deionized water, freeze-dried, placed in a dessicator, and re-weighed (cf. Magni & Montani, 2000). Although both oven-drying and freeze-drying can remove moisture, we applied the freeze-drying method to avoid the potential loss of any volatile compounds on the filter, which can occur with oven-drying. TSS concentrations were calculated from the weight increases on the same filters before and after filtration. Duplicate TSS samples were analyzed, and the mean coefficient of variation from the duplicate measurements was about 14%.

Total suspended solids (TSS) consist of tripton and phytoplankton. We subtracted the dry weight (DW) of phytoplankton from TSS to yield tripton concentration (cf. Philips et al., 1995). Dry weight of phytoplankton in each sample was then estimated from the Chl *a* by assuming a C/Chl *a* of 56 (Tada & Morishita, 1997) and a DW/C of 2.5 (Montani, 1990), which were previously reported in the eastern Seto Inland Sea. We thus used 140 as a conversion factor from Chl *a* to DW of phytoplankton ( $DW/Chl\ a = 56 * 2.5 = 140$ ).

### Components of light attenuation

To examine the relative contribution of each optically active component to  $K_d$ , it is generally assumed that  $K_d$  can be used to approximate a set of partial attenuation coefficients. Under this assumption, we partitioned  $K_d$  into several fractions:

$$K_d = K_w + K_{CDOM} + K_{TSS} \quad (4)$$

where  $K_w$ ,  $K_{CDOM}$ , and  $K_{TSS}$  are the partial attenuation coefficients due to seawater, CDOM, and TSS, respectively.  $K_{TSS}$  can be further divided into two fractions:

$$K_{TSS} = K_{PHY} + K_{TRI} \quad (5)$$

where  $K_{PHY}$  and  $K_{TRI}$  are the partial attenuation coefficients of phytoplankton measured as Chl *a* and tripton, respectively. In this study,  $K_w$  was set at a constant value of 0.038 m<sup>-1</sup> (Lorenzen, 1972). Furthermore, based on the results of Pfannkuche (2002),  $K_{CDOM}$  was estimated from the following equation (Lund-Hansen, 2004; Zhang et al., 2007):

$$K_{CDOM} = 0.221CDOM_{440} \quad (6)$$

where 0.221 is the specific absorption coefficient of  $CDOM_{440}$ .

To calculate  $K_{TSS}$ , we subtracted  $K_w + K_{CDOM}$  from  $K_d$ . We estimated the specific attenuation coefficient of Chl *a* (m<sup>2</sup> mg Chl *a*<sup>-1</sup>), based on the simple linear regression analysis between  $K_{TSS}$  (m<sup>-1</sup>) and the mean euphotic zone Chl *a* (mg m<sup>-3</sup>) during a 13-month period:

$$K_{TSS} = bChl-a + a \quad (7)$$

where  $a$  is the intercept and  $b$  is the specific attenuation coefficient of Chl *a* (=slope). We thereafter calculated  $K_{PHY}$  by multiplying the specific attenuation coefficient of Chl *a* by the mean euphotic zone Chl *a*. The remaining portion of  $K_{TSS}$ , which could not be explained by  $K_{PHY}$ , is defined as  $K_{TRI}$ . These estimation methods of  $K_{PHY}$  and  $K_{TRI}$  are fully explained and discussed in the Discussion.

## Results

### Temperature and salinity

Surface temperature showed a clear seasonal variation, with a minimum of 7.7°C in February and a maximum of 26.8°C in August (Fig. 2a). A thermocline (vertical differences in temperature >2.5°C) developed during the summer season (June–August). Except for these months, differences between the bottom and surface waters were within 1.8°C.

Salinity showed higher values in winter and spring (December–May), and lower values in summer and autumn (June–November) (Fig. 2b). A halocline (vertical differences of salinity >0.8) developed in June and September, with few observed differences in salinity in the vertical plane in other months.

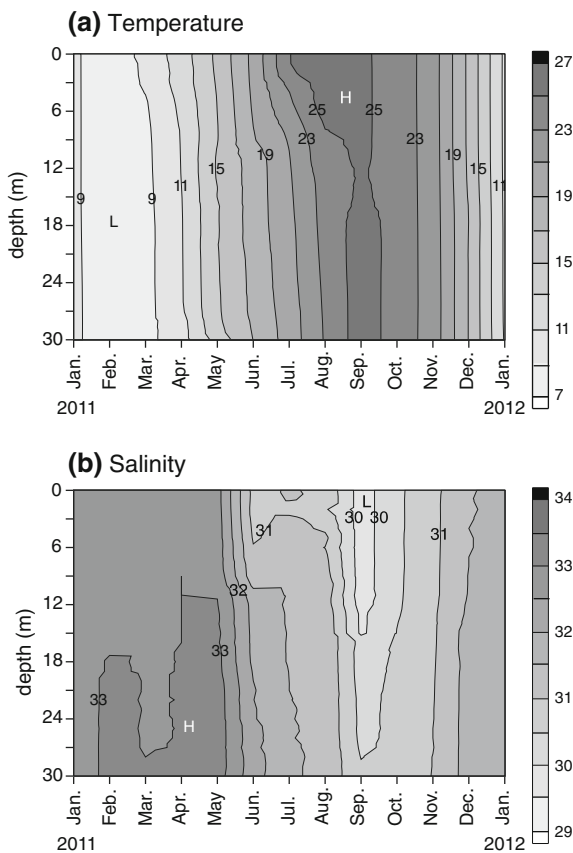


**Fig. 2** Vertical contour maps of **a** temperature and **b** salinity at the sampling location during the study period

**Total PAR attenuation**

The attenuation coefficient of PAR through the water column ( $K_d$ ) ranged from  $0.179 \text{ m}^{-1}$  in February to  $0.507 \text{ m}^{-1}$  in June, with a mean ( $\pm$ SD) for all data ( $n = 13$ ) of  $0.262 \pm 0.087 \text{ m}^{-1}$  (Fig. 3a). Although there was no clear seasonal trend,  $K_d$  was lower in spring (March–May) and higher in autumn (September–November). The highest value occurred in June, a month of high precipitation during the early summer season.

**Light attenuation due to CDOM, seawater, and particles**

The water column CDOM absorption coefficient at 440 nm was lower in winter and spring, but higher in summer and autumn (Fig. 4a). In most months, there

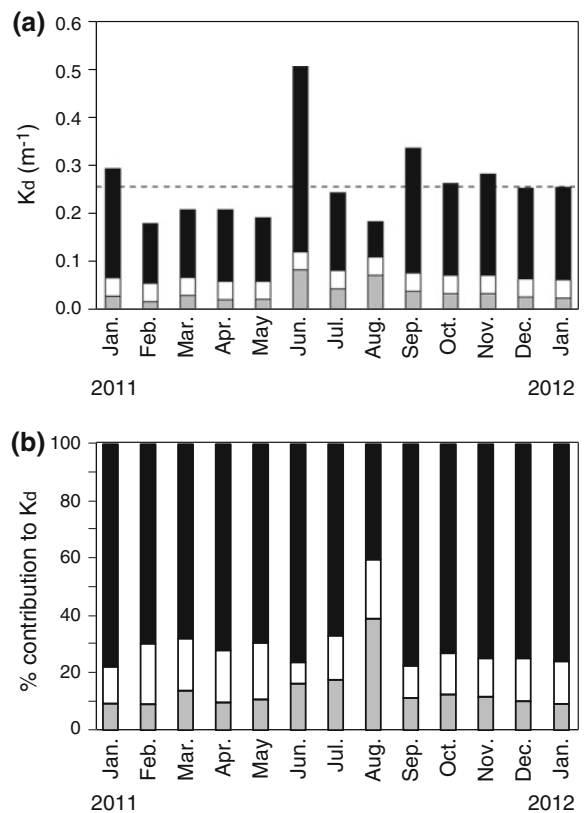


**Fig. 3** **a** Temporal variation in the PAR-attenuation coefficient through the water column ( $K_d$ ) during the sampling period. Grey, white, and black bars show the partial attenuation coefficients due to CDOM ( $K_{CDOM}$ ), seawater ( $K_w$ ), and suspended particles ( $K_{TSS}$ ), respectively. Light attenuation due to seawater was set as a constant value of  $0.038 \text{ m}^{-1}$ . The dashed line indicates the mean value of  $K_d$  through the study period ( $0.262 \text{ m}^{-1}$ ). Note that the light attenuation due to CDOM in January 2011 was estimated from the salinity (see text). **b** Percentage contributions of the  $K_{CDOM}$ ,  $K_w$ , and  $K_{TSS}$  to the  $K_d$  at each sampling time

was little vertical stratification in  $CDOM_{440}$  (up to  $0.092 \text{ m}^{-1}$ ). However, in June, the  $CDOM_{440}$  had an extremely high value of  $0.622 \text{ m}^{-1}$  at the surface, and decreased rapidly with depth. There was a significant inverse relationship between  $CDOM_{440}$  and salinity ( $CDOM_{440} = -0.0399sal + 1.421$ ,  $r = -0.443$ ,  $P < 0.01$ ), indicating that  $CDOM_{440}$  could be used as a proxy for salinity, when  $CDOM_{440}$  is not known.

We calculated  $K_{CDOM}$  in the euphotic zone at each sampling time, based on the distribution of  $CDOM_{440}$  and temporal changes in  $Z_{eu}$  (Fig. 3a). The  $K_{CDOM}$  ranged from  $0.016 \text{ m}^{-1}$  in February to  $0.082 \text{ m}^{-1}$  in June, with a mean of  $0.035 \pm 0.020 \text{ m}^{-1}$ . Although

the contribution of  $K_{\text{CDOM}}$  to  $K_d$  reached 39% in August, the percentages varied from 9 to 18% in other months (Fig. 3b). The mean contribution of  $K_{\text{CDOM}}$  to  $K_d$  through the study period was 13%.

Likewise,  $K_w$ , which was taken to be a constant of  $0.038 \text{ m}^{-1}$ , accounted for a relatively small proportion of  $K_d$  (Fig. 3a), ranging from 8 to 21%, with a mean of 15% (Fig. 3b).

Consequently, PAR attenuation due to suspended particles ( $K_{\text{TSS}}$ ) was the predominant constituent of  $K_d$  among the three components (Fig. 3), ranging from 68 to 78%, except for in August (40%) (Fig. 3b).  $K_{\text{TSS}}$  accounted for a mean of approximately 70% of total PAR attenuation. Linear regression analysis yielded a strong relationship between  $K_{\text{TSS}}$  and  $K_d$ ;  $K_d = 1.107K_{\text{TSS}} + 0.053$  ( $r = 0.978$ ,  $P < 0.01$ ). The intercept value of 0.053 in the regression analysis was nearly equal to the mean of  $K_w + K_{\text{CDOM}}$  ( $0.038 + 0.035 = 0.073$ ) during the study period.

#### Variation of TSS, Chl *a*, and tripton

The distribution of TSS in the euphotic zone was similar to that of Chl *a*, rather than tripton (Fig. 4b–d). In contrast, the distribution pattern of TSS in the aphotic zone (where there was less than 1% of surface PAR) coincided well with that of tripton. Both Chl *a* and tripton thus affected the variations in TSS in the water column.

Phytoplankton biomass, measured as Chl *a*, was highly variable during the sampling period (Fig. 4c). For instance, from February to May, concentrations of  $<1.5 \text{ mg m}^{-3}$  were recorded throughout the water column, whereas extremely high values, over  $8.0 \text{ mg m}^{-3}$  and up to  $11.4 \text{ mg m}^{-3}$  were observed in the upper layer ( $<5 \text{ m}$ ) in June.

In contrast to the large variations in phytoplankton biomass, tripton concentrations were relatively stable, both temporally and vertically (Fig. 4d). Tripton concentration varied from  $0.05$  to  $2.75 \text{ g m}^{-3}$ , and 85% (55 of 65 cases) of the measurements were within a narrow range between  $0.50$  and  $1.50 \text{ g m}^{-3}$ .

We examined the relationships between suspended particles (i.e., TSS, Chl *a*, and tripton) and PAR attenuation during the sampling period (Fig. 5). There was a significantly strong relationship between mean Chl *a* in the euphotic zone and both the  $K_{\text{TSS}}$  and  $K_d$  ( $P < 0.01$ ) (Fig. 5b, e). The relationship between

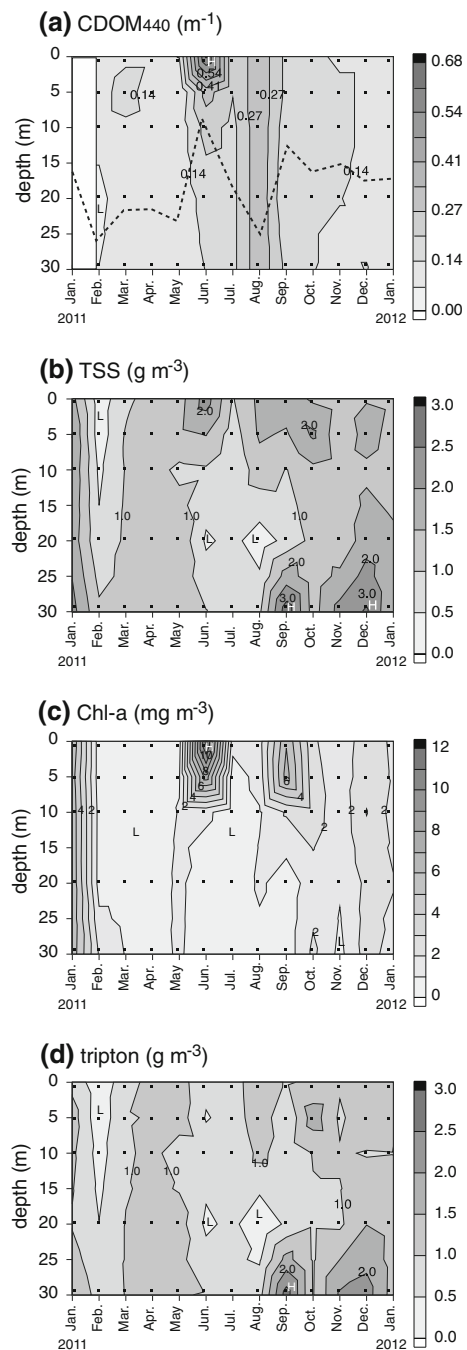


**Fig. 4** Vertical contour maps of **a** absorption coefficient of filtered seawater at 440 nm wavelength ( $\text{CDOM}_{440}$ ), concentrations of **b** total-suspended solids (TSS), **c** chlorophyll *a* (Chl *a*), and **d** tripton during the study period. Euphotic depth is denoted by the dashed line in the  $\text{CDOM}_{440}$  contour

mean TSS in the euphotic zone and the  $K_{\text{TSS}}$  was also significant ( $P < 0.05$ ) (Fig. 5a). Although not statistically significant ( $P = 0.06$ ), water with a higher

mean TSS tended to show higher  $K_d$  values (Fig. 5d). Conversely, there was no clear relationship between mean tripton concentration in the euphotic zone and both  $K_{TSS}$  and  $K_d$  ( $P > 0.05$ ) (Fig. 5c, f).

## Discussion

### Causes of PAR attenuation under average conditions

Our results suggest that CDOM (13%) and seawater (15%) are minor components of total PAR attenuation (100%) in our study area under average conditions (Fig. 3b). Consequently, most PAR attenuation (72%) is due to suspended particles. In contrast, CDOM or CDOM + seawater have been identified as primary contributors to total PAR attenuation in some turbid brackish waters (McPherson & Miller, 1994; Xu et al., 2005; Obrador & Pretus, 2008). Our study, however, is in agreement with previous studies, which emphasized the importance of suspended particles for total PAR attenuation in saline waters (e.g. McPherson & Miller, 1994; Devlin et al., 2008; Lin et al., 2009; Lund-Hansen et al., 2010b).

There was a significant positive relationship between  $K_{TSS}$  and the mean euphotic zone Chl *a* (Fig. 5b), and the resulting equation was as follows:

$$K_{TSS}(\text{m}^{-1}) = 0.031\text{Chl } a(\text{mg m}^{-3}) + 0.118 \quad (8)$$

By comparing Eq. (5) with Eq. (8), we are able to determine that the mean value of  $K_{TRI}$  during the sampling period is  $0.118 \text{ m}^{-1}$ . This constant may be attributable to the tendency of the specific attenuation coefficient of tripton ( $\text{m}^2 \text{ g tripton}^{-1}$ ) to decrease with increasing tripton concentration, in relation to changes in particle quality (e.g., particle size and shape). This explanation allows us to estimate  $K_{TRI}$  using a constant ( $0.118 \text{ m}^{-1}$ ). We can also deduce that the slope of Eq. (8) represents the specific attenuation coefficient for Chl *a* ( $\text{m}^2 \text{ mg Chl } a^{-1}$ ) (cf. Gallegos & Moore, 2000), and the contribution of phytoplankton to  $K_{TSS}$  is proportional to the mean euphotic zone Chl *a* concentration. Therefore, mean  $K_{PHY}$  is estimated as  $0.070 \text{ m}^{-1}$ , calculated from the 13-month mean Chl *a* concentration in the euphotic zone of  $2.26 \text{ mg m}^{-3}$ . These estimates indicate that  $K_{TRI}$  and  $K_{PHY}$  account for 45 and 27% of the  $K_d$  (mean =  $0.262 \text{ m}^{-1}$ ), respectively, showing that under average conditions

total PAR attenuation in the study area is primarily caused by tripton.

The aforementioned specific attenuation coefficient for Chl *a*,  $0.031 \text{ m}^2 \text{ mg Chl } a^{-1}$ , is within the range of previously reported values (e.g., Lorenzen, 1972; McPherson & Miller, 1994; Christian & Sheng, 2003; Lund-Hansen, 2004). Furthermore, this value is very similar to the coefficient value obtained in western Seto Inland Sea by Hashimoto & Tada (1994),  $0.034 \text{ m}^2 \text{ mg Chl } a^{-1}$ . We can thus regard the estimated  $K_{PHY}$  as a reasonable one. However, it must be noted that our estimation method of  $K_{PHY}$  has two weaknesses. First, we analyzed Chl *a* using the trichromatic method of Jeffrey & Humphrey (1975). This method tends to overestimate the Chl-*a* by, on average, 20% in Harima Sound, mainly owing to the presence of phaeo-pigments in the seawater (Yamaguchi et al., 2012). Second, we estimated the specific attenuation coefficient of Chl *a* by linear regression analysis, which implies that the obtained value includes the influences of some materials, which covary with Chl *a*. It might therefore be considered that the  $K_{PHY}$  obtained in this study produces a PAR-attenuation coefficient derived from phytoplankton and some phytoplankton remnants. If so, the estimated mean contribution of  $K_{PHY}$  to  $K_d$  (27%) should be regarded as an upper level. This in turn suggests that we may have underestimated the contribution of tripton as a shading component (45%).

Tripton is generally divided into non-living organic and inorganic particles. In the ocean, the non-living organic component consists of fragments of dead organisms, including phytoplankton. In coastal areas, the inorganic particles are mainly derived from suspended sediments such as silt and clay (Obrador & Pretus, 2008). There was no clear relationship between concentrations of Chl *a* and tripton in the euphotic zone (Fig. 4), with the correlation coefficient between them nearly equal to zero ( $r = -0.103$ ,  $P > 0.05$ ). Although we could not separate the tripton into organic and inorganic fraction, the lack of relationship between Chl *a* and tripton may suggest that inorganic particles account for the main portion of tripton.

According to previous field studies from semi-enclosed coastal areas, the mean relative contributions of  $K_{TRI}$  to total PAR attenuation was higher than that of  $K_{PHY}$  in Arhus Bay, Kattegat (Lund-Hansen, 2004), Florida Bay (Phlips et al., 1995; Kelble et al., 2005),

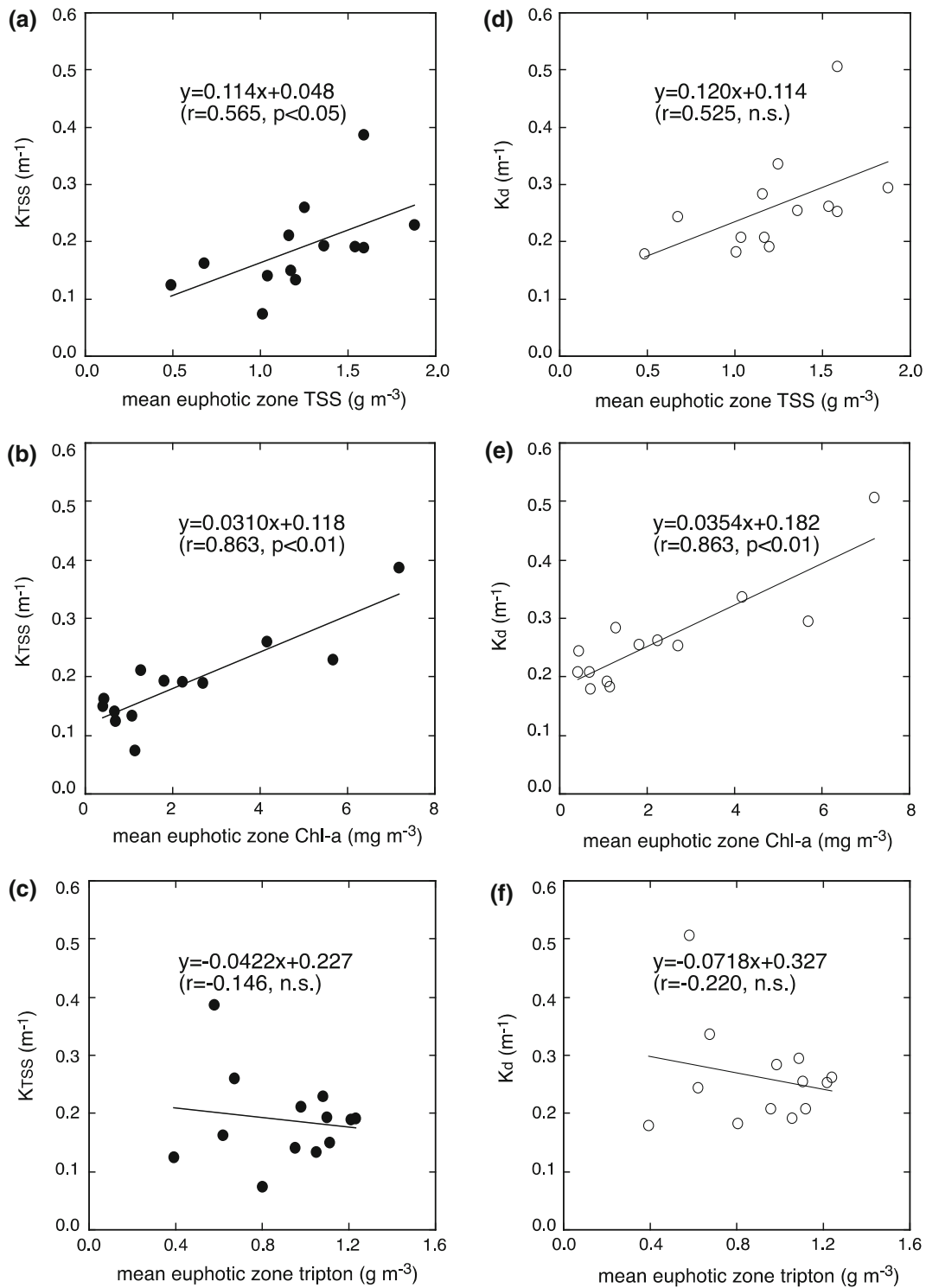


**Fig. 5** Relationships of PAR-attenuation coefficients due to suspended particles ( $K_{TSS}$ ) with the respective concentrations of mean euphotic zone **a** total-suspended solids (TSS), **b** chlorophyll

**a** (Chl *a*), and **c** tripton, and total PAR-attenuation coefficient ( $K_d$ ) with the concentrations of mean euphotic zone **d** TSS, **e** Chl *a*, and **f** tripton



Tampa Bay and Charlotte Harbor (McPherson & Miller, 1987; McPherson & Miller, 1994), Yellow Sea (Lin et al., 2009), while few studies found the dominance of the  $K_{PHY}$  as compared with the  $K_{TRI}$  (e.g., Obrador & Pretus, 2008). Considering both our results and previous studies, we suggest that tripton is generally more important than phytoplankton as a shading component in semi-enclosed coastal areas, although further studies are necessary.

#### Temporal variation of PAR attenuation

As previously discussed, our results emphasize that total PAR attenuation ( $K_d$ ) in the study area is primarily caused by light attenuation due to tripton ( $K_{TRI}$ ) under average conditions. In contrast, monthly variation of  $K_d$  was highly correlated with mean euphotic zone phytoplankton concentration, rather than tripton (Fig. 5e, f). According to the coefficient of determination ( $r^2$ ), phytoplankton explained 75% of the variability in  $K_d$  (Fig. 5e). These facts demonstrate that phytoplankton is the main driver of temporal variability in light environments in the study area, even though it only accounts for 27% of  $K_d$  under average conditions. In our study area, the relative standard deviation (RSD) of the mean Chl *a* concentration in the euphotic zone during the sampling period was 95%. This value was far larger than that of tripton (30%, Fig. 4c, d). The large difference in the variability between Chl *a* and tripton implies that Chl *a* is the main cause of  $K_d$  variability.

The reason for the insignificant relationship between  $K_d$  and the mean euphotic zone tripton concentration is unclear (Fig. 5f). We measured the tripton concentration in terms of dry weight (DW), and did not examine its particle size or other aspects, such as particle shape and refractive index, which are more important for PAR attenuation than DW (Baker & Lavelle, 1984; McPherson & Miller, 1987; Lund-Hansen et al., 2010a). Furthermore, we calculated the concentration of tripton by subtracting the DW of phytoplankton from TSS. Such restrictions may affect the correlation between PAR attenuation and tripton concentration. However, given the high coefficient of determination between  $K_d$  and Chl *a* (Fig. 5e), phytoplankton is clearly of prime importance to the temporal variation of  $K_d$ .

Obrador & Pretus (2008) examined the light regime and components of turbidity in the water column of

Alnufera des Grau, a Mediterranean coastal lagoon. They noted that temporal changes in total PAR attenuation were chiefly responsible for phytoplankton distribution, while the effect of phytoplankton on total PAR attenuation was less important than that of dissolved organic matter. Both our study and that of Obrador & Pretus (2008) indicate that the main component of light attenuation does not always govern the temporal variation of light attenuation in estuarine and coastal regions.

In the eastern Seto Inland Sea (including Harima Sound), phytoplankton biomass has decreased in recent years (Yamaguchi, 2008; Nishikawa et al., 2010). In relation to this symptom of “oligotrophication” (cf. Yamamoto, 2003), it is considered that water clarity has increased, and this trend will continue (e.g., Tarutani, 2007). However, the roles of phytoplankton and the quantitative impact of phytoplankton decrease on the light environment have not yet been studied in this region. Our results suggest that water clarity in the offshore area of the eastern Sea will gradually increase, due to a decrease in phytoplankton biomass (Yamaguchi, 2008; Nishikawa et al., 2010). This is because phytoplankton are a main driver of temporal variability in total PAR attenuation. However, the magnitude of the changes in water clarity may be relatively small, no more than 30%, since the contribution of phytoplankton to total PAR attenuation is not high. Such estimates will be meaningful for predicting future ecosystem changes in the eastern Seto Inland Sea.

#### Conclusion

This study examined (1) the causes of total PAR attenuation ( $K_d$ ) and (2) the driving force of its temporal variation in Harima Sound in Japan. Our study concludes as follows: (1) The main component of  $K_d$  in the offshore region of this area is PAR attenuation due to tripton ( $K_{TRI}$ ), accounting for at least 45% of  $K_d$  on average. (2) The temporal variability of  $K_d$ , is chiefly responsible for PAR attenuation due to phytoplankton ( $K_{PHY}$ ), which explains 75% of the variability in  $K_d$ . These two major conclusions suggest that the main component of total PAR attenuation does not always govern the temporal variation of PAR attenuation in coastal regions.

**Acknowledgments** We thank the members of the laboratory of Marine Environmental Studies, Kagawa University, and Mr. K. Kishimoto, captain of the RV *Calanus* III, for their generous assistance with sampling. We thank Dr. L. Wicks for checking the English text. We are also grateful to Dr. L. Naselli-Flores and two anonymous reviewers for their constructive comments. This work was supported by JSPS KAKENHI Grant No. 24780187 and 23310007. A part of this work was also supported by a grant, “Coastal Ecosystem Complex”, from the Japanese Ministry of Education, Culture, Sports, Science and Technology.

## References

- Association for the environmental conservation of the Seto Inland Sea, 2010. Environmental Conservation for the Seto Inland Sea (in Japanese). Environmental Agency of Japan, Tokyo.
- Baker, E. T. & J. W. Lavelle, 1984. The effect of particle size on the light attenuation coefficient of natural suspensions. *Journal of Geophysical Research: Oceans* 86: 8197–8203.
- Baker, K. S. & R. C. Smith, 1979. Quasi-inherent characteristics of the diffuse attenuation coefficient for irradiance. *Proceedings of SPIE volume 208, Ocean Optics VI*: 60–63.
- Branco, A. B. & J. N. Kremer, 2005. The relative importance of chlorophyll and colored dissolved organic matter (CDOM) to the prediction of the diffusive attenuation coefficient in shallow estuaries. *Estuaries* 28: 643–652.
- Christian, D. & Y. P. Sheng, 2003. Relative influence of various water quality parameters on light attenuation in Indian River Lagoon. *Estuarine, Coastal and Shelf Science* 57: 961–971.
- Cloern, J. E., B. E. Cole, R. L. J. Wong & A. E. Alpine, 1985. Temporal dynamics of estuarine phytoplankton: a case study of San Francisco Bay. *Hydrobiologia* 129: 153–176.
- Devlin, M. J., J. Barry, D. K. Mills, R. J. Gowen, J. Foden, D. Sivyer & P. Tett, 2008. Relationships between suspended particulate material, light attenuation and Secchi depth in UK marine waters. *Estuarine, Coastal and Shelf Science* 79: 429–439.
- Foden, J., D. B. Sivyer, D. K. Mills & M. J. Devlin, 2008. Spatial and temporal distribution of chromophoric dissolved organic matter (CDOM) fluorescence and its contribution to light attenuation in UK waterbodies. *Estuarine, Coastal and Shelf Science* 79: 707–717.
- Fujiwara, T., 2010. Oceanographic characteristics affecting nutrient distribution and biological productivity in Harima-Nada. *Setonaikai* 59: 4–9. (in Japanese).
- Gallegos, C. L. & K. Moore, 2000. Factors contributing to water-column light attenuation. In Batiuk, R. A., et al. (eds), *Chesapeake Bay Submerged Aquatic Vegetation Water Quality and Habitat-based Requirements and Restoration Targets: A Second Technical Synthesis*. US Environmental Protection Agency, Annapolis: 35–54.
- Hashimoto, T. & K. Tada, 1994. Optical properties of sea water in Hiroshima Bay, Japan. *Oceanography in Japan* 6: 151–155. (in Japanese with English abstract).
- Jeffrey, S. W. & G. F. Humphrey, 1975. New spectrophotometric equations for determining chlorophylls a, b,  $c_1$  and  $c_2$  in higher plants, algae and natural phytoplankton. *Bi-ochimie und Physiologie der Pflanzen* 167: 191–194.
- Kelble, C. R., P. B. Ortner, G. L. Hitchcock & J. N. Boyer, 2005. Attenuation of photosynthetically available radiation (PAR) in Florida Bay: potential for light limitation of primary producers. *Estuaries* 28: 560–571.
- Kirk, J. T. O., 2011. *Light and Photosynthesis in Aquatic Ecosystems*, 3rd ed. Cambridge University Press, Cambridge.
- Laanen, M. L., S. W. M. Peters, A. G. Dekker & H. J. van der Woerd, 2011. Assessment of the scattering by sub-micron particles in inland waters. *Journal of the European Optical Society: Rapid Publications* 6: 11046.
- Lin, S., T. Zou, H. Gao & X. Guo, 2009. The vertical attenuation of irradiance as a function of turbidity: a case of Huanghai (Yellow) Sea in spring. *Acta Oceanologica Sinica* 28: 66–75.
- Lorenzen, C. J., 1972. Extinction of light in the ocean by phytoplankton. *Journal du Conseil Permanent International pour l’Exploration de la Mer* 34: 262–267.
- Lund-Hansen, L. C., 2004. Diffuse attenuation coefficients  $K_d(\text{PAR})$  at the estuarine North Sea-Baltic Sea transition: time-series, partitioning, absorption, and scattering. *Estuarine, Coastal and Shelf Science* 61: 251–259.
- Lund-Hansen, L. C., T. J. Andersen, M. H. Nielsen & M. Pejrup, 2010a. Suspended matter, chl- $a$ , CDOM, grain sizes, and optical properties in the arctic fjord-type estuary, Kangerlussuaq, west Greenland during summer. *Estuaries and Coasts* 33: 1442–1451.
- Lund-Hansen, L. C., D. N. Hai, N. N. Lam & M. H. Nielsen, 2010b. Optical properties of a tropical estuary during wet and dry conditions in the Nha Phu estuary, Khanh Hoa Province, south-east Vietnam. *Hydrobiologia* 644: 207–216.
- Magni, P. & S. Montani, 2000. Water chemistry variability in the lower intertidal zone of an estuary in the Seto Inland Sea, Japan: seasonal patterns of nutrients and particulate compounds. *Hydrobiologia* 432: 9–23.
- Manabe, T., M. Tanda, Y. Hori, S. Nagai & Y. Nakamura, 1994. Changes in eutrophication and phytoplankton in Harima-Nada – results of environmental monitoring for 20 years. *Bulletin on Coastal Oceanography* 31: 169–181. (in Japanese with English abstract).
- McMahon, T. G., R. C. T. Raine, T. Fast, L. Kies & J. W. Patching, 1992. Phytoplankton biomass, light attenuation and mixing in the Shannon estuary, Ireland. *Journal of the Marine Biological Association of the United Kingdom* 72: 709–720.
- McPherson, B. F. & R. L. Miller, 1987. The vertical attenuation of light in Charlotte Harbor, a shallow, subtropical estuary, south-western Florida. *Estuarine, Coastal and Shelf Science* 25: 721–737.
- McPherson, B. F. & R. L. Miller, 1994. Causes of light attenuation in Tampa Bay and Charlotte Harbor, southwestern Florida. *Water Resources Bulletin* 30: 43–53.
- Monbet, Y., 1992. Control of phytoplankton biomass in estuaries: a comparative analysis of microtidal and macrotidal estuaries. *Estuaries* 15: 563–571.
- Montani, S., 1990. Dynamics of suspended particles. In Yanagi, T. (ed.), *The Science of Shiome* (in Japanese). Koseisha-Koseikaku Press, Tokyo: 50–67.
- Nelson, N. B., D. A. Siegel & A. F. Michaels, 1998. Seasonal dynamics of colored dissolved material in the Sargasso Sea. *Deep-Sea Research I* 45: 931–957.

- Nishikawa, T., Y. Hori, S. Nagai, K. Miyahara, Y. Nakamura, K. Harada, M. Tanda, T. Manabe & K. Tada, 2010. Nutrient and phytoplankton dynamics in Harima-Nada, eastern Seto Inland Sea, Japan during a 35-year period from 1973 to 2007. *Estuaries and Coasts* 30: 417–427.
- Obrador, B. & J. L. Pretus, 2008. Light regime and components of turbidity in a Mediterranean coastal lagoon. *Estuarine, Coastal and Shelf Science* 77: 123–133.
- Parsons, T. R., M. Takahashi & B. Hargrave, 1984. *Biological Oceanographic Processes*, 3rd ed. Pergamon Press, Oxford.
- Pfannkuche, J., 2002. Optical properties of Otago shelf waters: South Island New Zealand. *Estuarine, Coastal and Shelf Science* 55: 613–627.
- Phlips, E. J., T. C. Lynch & S. Badylak, 1995. Chlorophyll *a*, tripton, color, and light availability in a shallow tropical inner-shelf lagoon, Florida Bay, USA. *Marine Ecology Progress Series* 127: 223–234.
- Suksomjit, M., S. Nagao, K. Ichimi & K. Tada, 2009. Variation of dissolved organic matter and fluorescence characteristics before, during and after phytoplankton bloom. *Journal of Oceanography* 65: 835–846.
- Tada, K. & K. Morishita, 1997. The changes of environmental chemical conditions and biomass on lower trophic levels in a coastal bay. *Technical Bulletin of Faculty of Agriculture, Kagawa University* 49: 35–47. (in Japanese with English abstract).
- Tarutani, K., 2007. Long-term variations in water environments in the Seto Inland Sea of Japan during 1973–2002 based on data from the fisheries monitoring program. *Japanese Journal of Benthology* 62: 52–56. (in Japanese with English abstract).
- Xu, J., R. R. Hood & S.-Y. Chao, 2005. A simple empirical optical model for simulating light attenuation variability in a partially mixed estuary. *Estuaries* 28: 572–580.
- Yamaguchi, H., 2008. Long-term variation of phytoplankton biomass in Osaka Bay reconstructed from previous data. *Setonaikai* 54: 21–25. (in Japanese).
- Yamaguchi, H., S. Montani, H. Tsutsumi, K. Hamada, N. Ueda & K. Tada, 2007. Dynamics of microphytobenthic biomass in a coastal area of western Seto Inland Sea, Japan. *Estuarine, Coastal and Shelf Science* 75: 423–432.
- Yamaguchi, H., R. Katahira, Y. Ogata, M. Shiraiishi, K. Ichimi & K. Tada, 2012. Comparison of fluorometric and spectrophotometric methods for determination of chlorophyll-*a* in coastal seawater samples. *Sea and Sky* 88: 49–56.
- Yamamoto, T., 2003. The Seto Inland Sea—eutrophic or oligotrophic? *Marine Pollution Bulletin* 47: 37–42.
- Zhang, Y., B. Zhang, R. Ma, S. Feng & C. Le, 2007. Optically active substances and their contributions to the underwater light climate in Lake Taihu, a large shallow lake in China. *Fundamental and Applied Limnology* 170: 11–19.